Experimental research of temperature sensor based on twin-core fiber

Ruifeng Zhao (赵瑞峰)[1,2], Li Pei (裴 丽)[1,2*], Zhuoxuan Li (李卓轩)[1,2], Tigang Ning (宁提纲)[1,2], Linyong Fan (范林勇)[1,2], and Weiwei Jiang (江微微)[1,2]

[1]*Institute of Lightwave Technology, Beijing Jiaotong University, Beijing 100044, China*

[2]*Key Laboratory of All Optical Network and Advanced Telecommunication Network of Ministry of Education, Beijing Jiaotong University, Beijing 100044, China*

**Corresponding author: lipei@bjtu.edu.cn*

Received December 30, 2010; accepted January 31, 2011; posted online April 29, 2011

A low-cost, compact, and lossless temperature sensor based on a twin-core fiber (TCF) is demonstrated and manufactured by splicing two single-mode fibers to the ends of a TCF. The extinction ratio of the comb transmission spectrum is bigger than 15 dB, and the temperature sensitivity of the coupling angle is –0.02 rad/(°C· m) at –30–90 °C and –0.032 rad/(°C· m) at 90–175 °C. Finite element method is used to calculate the supermodes of the TCF, and the result agrees well with the experiment.

OCIS codes: 280.0280, 280.6780.

doi: 10.3788/COL201109.062801.

Compared with traditional dual-fiber sensors[1], the use of in-fiber optical sensors has increased rapidly due to their compact configuration. In-fiber optical sensors could be categorized in two classes: fiber Bragg grating (FBG) sensors and interferential sensors. FBG sensors have extensive applications because of their easy multiplexing and mature fabrication process. However, unlike in-fiber optical interferential sensors, the temperature sensitivity of FBG sensors is limited by the intrinsic refractive index temperature coefficient of fused silica[2]. Their lifetime is only decades because of the degradation in performance[3]. One of the potential candidates of in-fiber optical interferential sensors is made of dual-core fiber. This fiber is composed of two single-mode cores surrounded by common cladding, and has been used to implement in-fiber Michelson[4] and Mach-Zehnder[5] interferometers where light propagates in the two cores independently. If the two cores are identical, the dual-core fiber is also called a twin-core fiber (TCF). In addition, if the separation distance of the two cores is sufficiently small, complete energy exchange between the two cores of TCF occurs and the coupling angle is determined by

$$\phi = CL, \tag{1}$$

where C is the coupling coefficient in weak coupled-mode theory and L is the length of TCF. The coupling coefficient is usually determined by the optical wavelength and the refractive index profile of the TCF. The coupling coefficient and the TCF length both vary with temperature. The net effect is a change in the coupling angle.

In this letter, a compact in-fiber temperature sensor is fabricated by splicing two single-mode fibers (SMFs) to the ends of a piece of TCF. According to the weak coupled-mode theory, the fundamental mode of the output SMF in Fig. 1(a) is excited with the power of

$$P_{\mathrm{o}} \approx P_{\mathrm{i}} \left[1 - \sin^2(\phi)\right], \tag{2}$$

where P_{i} is the power illuminated to the input SMF. A high-quality comb transmission spectrum is obtained. The insertion loss is sufficiently slight to be neglected. An operating temperature range from –30 to 175 °C is tested, and the temperature sensitivity of the coupling angle is obtained. Finite element method (FEM) is used to calculate the propagation constants of the two supermodes, and the result is consistent with the comb transmission spectrum of the experiment. The temperature sensitivity is interpreted by the temperature coefficient of the propagation constant of the two supermodes.

The TCF preform was first prepared by filling a side-grooved, large-diameter pure silica rod with two identical small-diameter Ge-doped silica rods and other small-diameter pure silica rods. These were fixed in a pure silica tube. The in-fiber temperature sensor was then fabricated, as shown in Fig. 1(a). Compared with the traditional side-polishing and attaching method[6], the proposed method is simple, flexible, and low-cost. Figure 1(b) shows the cross-section microscopy image of the TCF. The cores were designed to have identical refractive index and diameter; however, they lost their original round shape during the drawing process. The deformation could be suppressed by filling the gap of the preform with pure silica rods of much smaller diameter. Nonuniformities of the two cores affect the coupling properties of TCF[7]. However, the high extinction ratio of the comb transmission spectrum in Fig. 2 shows that the solid TCF has good coupling properties, despite core deformation. Neither of the cores was designed to be at the center of the fiber cross section, and the SMF core could be connected with any of the TCF cores. A commercial fusion splicer was used to splice the SMF and the TCF by manual operation and special splicer setting. The transmission power was monitored during the splicing operation to ensure lossless splicing between SMF core and one of the TCF cores. Figure 2 shows that the insertion loss of the sensor is very small and negligible. A significant drop is found in the spectrum near 1380 nm because of the high concentration of OH^- in the fiber induced during the fabrication and the strong optical

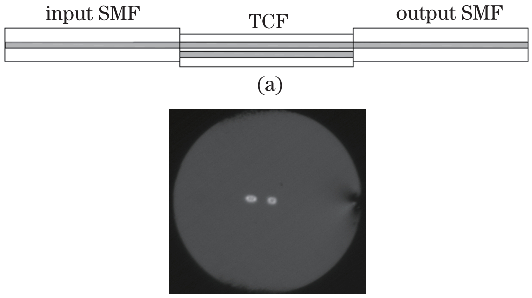

Fig. 1. (a) Schematic of the sensor; (b) cross section of the TCF.

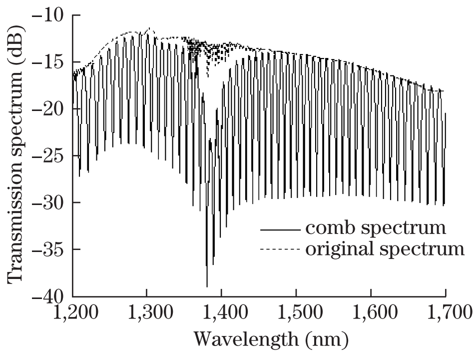

Fig. 2. Original spectrum of the super continuum laser source and comb output spectrum of the sensor.

absorption of OH^-around the wavelength.

In the experiments, two pieces of Corning SMF-28e+ optical fiber were fusion-spliced to each of the two ends of the TCF. For the TCF, the molar ratio of GeO_2 and SiO_2 in the cores was 0.0271, the radius of the cores was 2.86 μm, the separation distance between the two cores was 14.37 μm, the cladding diameter was approximately 130 μm, and the length of the TCF was approximately 40 cm. A Koheras supercontinuum white light laser was used as the input source. A Yokogawa AQ6375 optical spectrum analyzer was used to measure the comb transmission spectrum with the wavelength ranging from 1400 to 1700 nm. Figure 3 only shows the transmission spectrum from 1470 to 1510 nm because of the dense comb curve. It also shows that the wavelength shift is positive with the rising temperature. This means that the coupling angle is decreased because the coupling angle is approximately proportional to the wavelength.

Weak coupled-mode theory is usually applied to explain the coupling process in the TCF. However, the modal interference method is actually more accurate, especially when the two cores are very close. FEM is used to calculate the propagation constant and the mode field of the two orthogonal supermodes (i.e., eigenmodes) in the TCF because it has been successfully applied to simulate various complex photonic crystal fibers. At the input splice, two supermodes are excited with approximately equal power, whereas the even mode has a bigger propagation constant than the odd mode. Thus, a phase difference is formed at the output splice, and the coupling coefficient of the weak coupled-mode theory could be redefined as

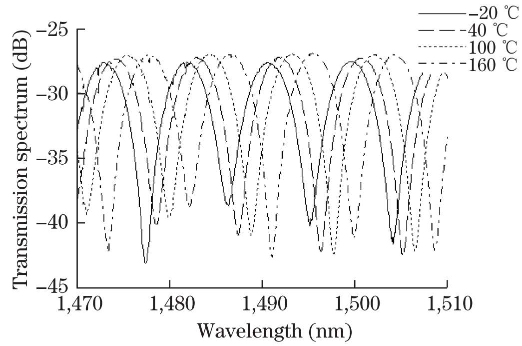

Fig. 3. Transmission spectra of the sensor when the temperature is –20, 40, 100, and 160 °C.

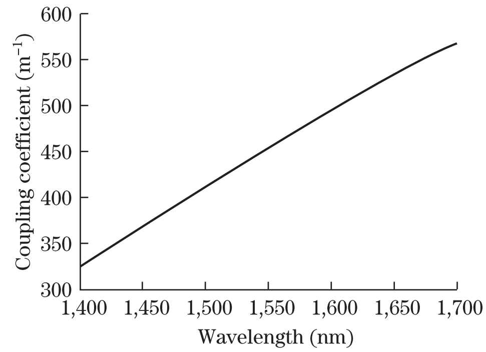

Fig. 4. Coupling coefficient of the TCF as a function of wavelength.

$$C = \frac{1}{2}\left(\beta_{\mathrm{e}} - \beta_{\mathrm{o}}\right), \tag{3}$$

where β_{e} and β_{o} are the propagation constant of the even mode and the odd mode, respectively. The coupling coefficient calculated by FEM is approximately linear in relation to the optical wavelength (Fig. 4). If one substitutes this to Eq. (2), a comb spectrum is obtained, consistent with the experimental result shown in Fig. 2.

Figure 5 shows the wavelength shift of the peak near 1500 nm. Although the fitted curve is quadratic, it remains approximately linear below or above 90 °C. The rate of peak wavelength shift to temperature change of unit length is

$$\frac{\mathrm{d}\lambda}{\mathrm{d}T \cdot L} = \begin{cases} 0.0568\ \mathrm{nm/(^\circ C \cdot m)}\ (T < 90\ ^\circ\mathrm{C}) \\ 0.0899\ \mathrm{nm/(^\circ C \cdot m)}\ (T > 90\ ^\circ\mathrm{C}) \end{cases}. \tag{4}$$

From Fig. 3, the rate of coupling angle change to wavelength shift is

$$\frac{\mathrm{d}\phi}{\mathrm{d}\lambda} = -0.354\ \mathrm{rad/nm}. \tag{5}$$

Substituting Eqs. (1), (3), and (4) to Eq. (5), the temperature sensitivity of the coupling angle becomes

$$\begin{aligned} \frac{\mathrm{d}\phi}{\mathrm{d}T \cdot L} &= \begin{cases} -0.020\ \mathrm{rad/(^\circ C \cdot m)} \quad (T < 90^\circ\mathrm{C}) \\ -0.032\ \mathrm{rad/(^\circ C \cdot m)} \quad (T > 90^\circ\mathrm{C}) \end{cases} \\ &= \frac{1}{2}\left(\frac{\mathrm{d}\beta_{\mathrm{e}}}{\mathrm{d}T} - \frac{\mathrm{d}\beta_{\mathrm{o}}}{\mathrm{d}T}\right) + \frac{1}{2}\left(\beta_{\mathrm{e}} - \beta_{\mathrm{o}}\right)\frac{\mathrm{d}L}{L\mathrm{d}T}. \end{aligned} \tag{6}$$

The second term at the right side of the equation originates from the thermal expansion of the fiber; its absolute value is much smaller than the first term. According to Eq. (2), the output power is a function of temperature

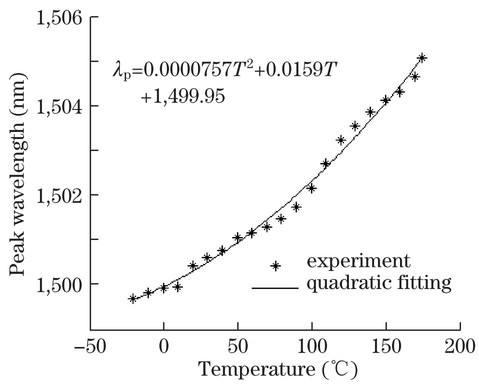

Fig. 5. Wavelength shift of a transmission peak near 1500 nm with temperature.

when the monochromatic light is illuminated to the input SMF, which is the sensing mechanism of the proposed temperature sensor based on TCF. From Eq. (6), the temperature sensitivity of the TCF sensor could be much higher than that of the FBG sensor because it is proportional to the length of the TCF.

In conclusion, the TCF is fabricated without any of the cores at the center of the cross section; however, it could be spliced with normal SMF without power loss. An in-fiber temperature sensor based on the interference of the two supermodes in TCF is demonstrated. The temperature sensitivity of low-cost, compact, and lossless in-fiber sensor is not a constant and could be calculated by analyzing the temperature coefficients of the propagation constants of the supermodes. This is because they dominate the temperature sensitivity of the sensor. The sensor also has potential application of high-temperature sensing because of its compact configuration and the good temperature resistance of silica.

This work was supported by the National Natural Science Foundation of China (Nos. 60837002 and 61007007), the Foundation for the Returning Scholars (No. [2008]890), the Ph.D. Programs Foundation of Ministry of Education of China (No. 200800040002), the Fundamental Research Funds for the Central Universities (No. 2011YJS007), and Beijing Jiaotong University Science and Technology Innovation Fund for Outstanding Doctoral (No. 141061522).

References

1. G. B. Hocker, Appl. Opt. **18,** 1445 (1979).
2. K. Li, Z. Zhou, and A. Liu, Chin. Opt. Lett. **7,** 121 (2009).
3. Y. J. Rao, Opt. Lasers Eng. **31,** 297 (1999).
4. L. Yuan, J. Yang, Z. Liu, and J. Sun, Opt. Lett. **31,** 2692 (2006).
5. L. Yuan, Z. Liu, J. Yang, and C. Guan, Opt. Express **16,** 4559 (2008).
6. P. Peterka, I. Kasik, J. Kanka, P. Honzatko, V. Matejec, and M. Hayer, IEEE Photon. Technol. Lett. **12,** 1656 (2000).
7. K. L. Reichenbach and C. Xu, Opt. Express **13,** 2799 (2005).